Structures and spectroscopic properties of sulfur-nitrogen-pnictogen chains : $R_2P-N=S=N-PR_2$ and $R_2P-N=S=N-AsR_2$

STRUCTURES AND SPECTROSCOPIC PROPERTIES OF SULFUR-NITROGEN-PNICTOGEN CHAINS: $R_2P–N=S=N–PR_2$ AND $R_2P–N=S=N–AsR_2$

Kristof M. Bal,[a] Julie Cautereels[b] and Frank Blockhuys[b]*

[a]*Department of Chemistry, University of Antwerp, Universiteitsplein 1, B-2610 Antwerpen, Belgium*

[b]*Department of Chemistry, University of Antwerp, Groenenborgerlaan 171, B-2020 Antwerpen, Belgium*

Dedicated to Prof. Georgiy Girichev on the occasion of his 70th birthday.

Abstract

The conformational and configurational preferences of $Me_2P–N=S=N–PMe_2$ (**3**) and $Me_2P–N=S=N–AsMe_2$ (**4**) have been identified using quantum chemical calculations at the DFT/B3LYP/6-311+G* level of theory. An approach in which energetic, structural (geometries and bond orders), electronic (analysis of the electron density) and spectroscopic properties are combined leads to the conclusion that these sulfur-nitrogen-pnictogen chains share many of the properties of their chalcogen-nitrogen analogues but that the through-space intramolecular interactions favouring the *Z,Z* configuration are even weaker than in these latter compounds. The results of this analysis also lead to an unambiguous assignment of the variable-temperature ^{31}P and ^{15}N NMR spectra of these compounds and their structures both in solution and in the solid state.

Keywords: Chalcogens, Pnictogens, Density functional calculations, Configuration determination, Intramolecular interactions

*Corresponding author. E-mail frank.blockhuys@uantwerpen.be.

1. Introduction

Sulfur-nitrogen compounds have shown to possess a unique and diverse chemistry, not only with respect to their properties but also to their reactivity, and this has made them the objects of a steadily increasing research effort since the late 1970s [1]. Undoubtedly, the interest of the chemical community in these systems was first generated by $(SN)_x$ polymer which, even though it does not contain any metal atoms, possesses metallic properties and displays superconductivity at low temperatures [2,3]. For some time these findings have been forming the basis of the idea that sulfur-nitrogen chains (polymers or oligomers) may have potential application as molecular wires for use in molecular electronics [4-7]. If so, it is clear that understanding the factors which are fundamental to the idea of molecular electrical conductivity – in particular π-delocalization which itself depends on the precise molecular configurations and conformations – becomes a central issue. This work logically starts with an investigation of the structural properties of model systems consisting of shorter sulfur-nitrogen chains, which are conventionally referred to as sulfur diimide derivatives (R–N=S=N–R'). In particular, acyclic structures containing the sulfur diimide fragment can, in the general case of two different substituents R and R' on the nitrogen atoms, adopt the four different configurations presented in Figure 1. In most cases the *E,E* isomer is destabilized with respect to the *Z,Z* and *E,Z* isomers; the energy difference between the latter two is usually small and the nature of R and R' determines which is the most stable [1,8,9]. An often-used back-of-the-envelope explanation for the relative instability of the *E,E* isomer is the effect of the interaction between the lone pairs on the nitrogen atoms. However, calculations on H–N=S=N–H at the B3LYP/aug-cc-pVQZ level of theory suggest that the N=S=N angles for *Z,Z*, *Z,E* and *E,E* are 123.9°, 115.6° and 109.9°, respectively [8,9]: repulsion between the lone pairs on nitrogen would lead to larger angles while the calculations suggest the opposite. This example clearly illustrates the basic challenges still ahead when dealing with the factors determining the configuration of sulfur diimides: the precise cause of these energy differences has not yet been definitively ascertained and these general trends have been observed mainly for systems in the solid state, *i.e.*, not for isolated molecules.

Structures in which R and R' are alkyl, aryl and organoelement substituents from Groups 14, 15 and 16 have been described and our own work on compounds with R = R' = SAr, SeAr has led to greater insight into the structural chemistry of such shorter chains [10-12]. What makes the chain compounds in which atoms of Group 15 are bonded to the nitrogen atoms of the sulfur diimide fragment particularly interesting is the fact that they can easily form transition metal complexes and a considerable number of mononuclear (chelate) and binuclear derivatives of $R_2X–N=S=N–XR_2$ (X = P, As, Sb and R = Me, ^{t}Bu, Ph) have been reported [13-22]; four of these have been structurally characterized using XRD [13-17]. The most studied compound in this group has been 1,1,5,5-tetra-*tert*-butyl-

3-thia-2,4-diaza-1,5-diphospha-2,3-pentadiene [$^{t}Bu_2P–N=S=N–P^{t}Bu_2$ (**1**), Figure 2] [23] of which the configuration in solution was investigated using NMR spectroscopy [24,25]: by comparing ^{15}N and ^{31}P chemical shifts of a set of reference compounds with the values found for **1**, Herberhold *et al.* derived that this compound primarily exists in a dynamic equilibrium of rapidly interconverting *Z,E* and *E,Z* isomers. If so, the configurational preference of **1** would be different from that of its Group-16 analogue Ph–S–N=S=N–S–Ph (**2**, Figure 2), of which the *Z,Z* isomer is the main (about 90%) component in solution [10]. Using the same technique Herberhold *et al.* assigned the ^{31}P singlet in the solid state to an *E,E* configuration, but this conclusion is debatable: in the crystal, the *E,E* configuration is known only for the sterically overcrowded Ar–N=Se=N–Ar derivative in which Ar = supermesityl [26]. Furthermore, related open-chain compounds containing the P–N=S=N–P fragment have only been found to display the *Z,E* configuration in the solid state [14,17,27], while *Z,Z* en *E,Z* configurations have been observed for compounds containing an X–N=S=N–X fragment with X = S, Se [10-12,28,29]; $Ph_2As–N=S=N–AsPh_2$ is also found in the *Z,Z* configuration [30].

It is clear that the final word on the configuration of sulfur-nitrogen-phosphorus chains such as **1** can not come from the results of experiments alone and there can be no doubt that quantum chemical calculations are capable of providing greater insight into these matters. To perform these calculations more efficiently **1** was replaced by a model system in which the *tert*-butyl groups were replaced by methyl groups, *i.e.*, 1,1,5,5-tetramethyl-3-thia-2,4-diaza-1,5-diphospha-2,3-pentadiene (**3**, Figure 2). A full configurational and conformational analysis was performed at the DFT/B3LYP/6-311+G* level of theory, and the geometries, energies and spectroscopic properties of all isomers and conformers of **3** were analyzed and correlated with the experimental results obtained in solution and in the solid state available in the literature. In addition, an analogous analysis was performed on the asymmetrical arsino derivative $Me_2P–N=S=N–AsMe_2$ (**4**, Figure 2), as a model for 1,1,5,5-tetra-*tert*-butyl-3-thia-2,4-diaza-1-phospha-5-arsa-2,3-pentadiene (**5**, Figure 2) and the results obtained for both **3** and **4** were compared in order to gauge the influence of the presence of the heavier pnictogen.

2. Computational details

All geometry optimizations were performed using the Gaussian 09 suite of programs [31] at the level of Density Functional Theory (DFT) using the B3LYP functional [32] and the 6-311+G* basis set [33-37] as it is implemented in the program. Harmonic frequency calculations were used to ascertain whether the optimized structures are minima on the Potential Energy Surface (PES). Chemical shielding factor values were calculated at the DFT/B3LYP/6-311+G* level of theory using the GIAO method [38-42] implemented in Gaussian 09. Chemical shifts of the phosphorus and nitrogen atoms were obtained by subtracting their calculated shielding values from the ones calculated for

their reference compounds, which are H_3PO_4 (C_3 symmetry) and CH_3NO_2, respectively, for which the shielding values are 293.4092 ppm and –152.4366 ppm [43], respectively, at the same level of theory. Topological analyses of (the Laplacian of) the total molecular electron density were performed using the AIM2000 program [44-46]. Bond orders were calculated according to the Hirshfeld scheme [47].

3. Results and discussion

In the following the configurations of the S=N double bonds will be differentiated using the *Z* and *E* labels, as usual. For the different conformers of the molecules, which are obtained by rotation around the X–N single bonds (X = P, As), the *syn* (*s*) and *anti* (*a*) labels will be used to mark the orientation of the lone pair on the X atoms in the parent compounds with respect to the P–N=S fragment, expressed by the torsion angles: the *syn* label will be used for torsion angles near 0° and the *anti* label for torsion angles near 180°. For orientations which clearly deviate from 0° or 180° the *gauche* (*g*) label will be used. When both peripheral $–XMe_2$ groups are in the *gauche* conformation they can be positioned at the same or at different sides of the molecule, which leads to different conformers with different energies; to differentiate them superscripts *s* and *a* are used in the former and latter cases, respectively (note that for gZZg only the *a* form exists). Figure 3 illustrates this for two such conformers of **4**. For the asymmetrical compound (**4**) the first two letters in the label always refer to the phosphorus atom, the final two to the arsenic atom.

3.1. $Me_2P–N=S=N–PMe_2$ (3): structure

Starting from the ten possible isomers and conformers of **3**, nine energy minima remained after geometry optimization: sZEs and aZEs converged into the same conformer and only one *Z*,*Z* isomer was found. From the relative energies of these conformers presented in Table 1 it is clear that the *Z*,*Z* conformer is energetically the most favourable. Three of the *E*,*Z* isomers lie less than 7 kJ.mol^{-1} higher, while a fourth *Z*,*E* isomer and the four *E*,*E* isomers have relative energies of more than 30 kJ.mol^{-1}. Based on these values the equilibrium conformer composition at 293 K for **3** is 78% gZZg, 11% gZEg^a, 6% gZEg^s and 5% gZEs, and this is in line with the one found for Ph–S–N=S=N–S–Ph (**2**) which is 89% *Z*,*Z* and 11% *Z*,*E* [10]. At room temperature gZZg will clearly be the dominant form in solution, which is consistent with the experimental vibrational frequencies of the N=S=N fragment in **3** [23] which fit best to the values calculated for the *Z*,*Z* isomer (Table 2).
The two conformers labelled gZEg^s and gEEg^s are related to the lower-energy structures with the gZEg^a and gEEg^a labels, respectively. The destabilization associated with both groups being located at the same side of the molecule is small, 1.65 kJ.mol^{-1} for gZEg and 0.22 kJ.mol^{-1} for gEEg, and considering that the second of these is so much smaller this is clearly due to a steric effect. The cal-

culated structures – those of gZZg, gZEg^a, gZEs and aZEg have been presented in Figure 4 – are clearly the result of the repulsive effect between the lone pairs on neighbouring nitrogen and phosphorus atoms: in all starting geometries in which these are positioned *syn* with respect to each other the phosphine group has been twisted away during the geometry optimization. For the phosphine groups in the *Z* position in the *Z,E* conformers the opposite conformation also poses a problem due to repulsion from the lone pair on the non-adjacent nitrogen atom. Therefore, in all these cases the lone pair on the phosphorus atom is positioned more or less orthogonally to the N=S=N plane leading to just one *gauche* interaction between the lone pair on nitrogen and one of the methyl groups. Only for aZEg this is not the case which explains the considerably higher energy of this structure. In gZZg the methyl groups are positioned orthogonally to the N=S=N plane and, consequently, the lone pairs on the two phosphorus atoms are oriented in a parallel fashion rather than in one line.

In an attempt to gain more insight into the possible reasons for these energy differences, the lone pairs on the various heteroatoms in **3** were identified as local concentrations in negative charge [(3,–3) critical points] in the negative of the Laplacian of the electron density ($-\nabla^2\rho$), according to the Quantum Theory of Atoms In Molecules (QTAIM) [44], and their orientations relative to the other fragments of the molecules were analyzed. In the gZEs conformer (Figure 4c), the P5 lone pair eclipses the S3–N4 bond, while in the gZEg^a conformer (Figure 4b) this lone pair has a *gauche* (and almost orthogonal) orientation with respect to both the N4 lone pair and the S3–N4 bond. Considering that within the VSEPR interpretation the repulsion between a lone pair and a bond is unfavourable, this can be used to explain the higher energy of the gZEs conformer compared to that of gZEg^a. This is supported by comparing the geometrical parameters of the gZEg and gZEs conformers, given in Table 3: the considerable elongation of the N4–P5 bond by 0.050 Å in the destabilized gZEs conformer does indeed also suggest a repulsive force due to the lone pair eclipsing the bond. A similar observation can be made for the aZEg conformer, in which the P1–N2 bond is elongated by about 0.030 Å compared to the values found for gZEg and gZEs, and, in this case, an eclipsation of the P1 and N2 lone pairs can be observed (Figure 4d). The considerably higher energy of this conformer compared to the other *Z,E* conformers can, however, not be attributed to repulsion between lone pairs alone, but also (and most likely mainly) to steric repulsion between the methyl groups on P1 and the lone pair on N4. This steric repulsion also explains the considerable widening of the P1–N2–S3 angle.

3.2. $Me_2P–N=S=N–PMe_2$ (3): NMR parameters

The relative energies in Table 1 suggest that the *Z,Z* configuration is the dominant species in solution for **3** (and **1**), but this is in contrast to the conclusions of Herberhold *et al.*, who suggested that the *Z,E* configuration is the most proficient species of **1** [24,25]. Their conclusions were exclusively

based on NMR spectroscopic measurements and trends in chemical shifts with respect to the configuration. The precise configuration **1** adopts in solution was dealt with in an NMR study: since no splitting of the ^{31}P singlet could be seen down to –100 °C, the authors could not exclude the possibility of just one "symmetric" form being dominantly present in solution [23]. Yet, for R = P(*t*-Bu)$_2$ and R' = PPh$_2$ a broadening and asymmetric splitting of the two ^{31}P singlets was observed below –100 °C; the behaviour of this particular compound was then ascribed to a dynamic *E*,*Z*/*Z*,*E* equilibrium in solution, in which one of the two isomers has a lower energy, which is expressed when the equilibrium is frozen [24]. A more comprehensive NMR study dealt with a series of compounds with R = P(*t*-Bu)$_2$ and different R' [25]. Based on a detailed analysis of chemical shifts and couplings a number of more or less general trends could be deduced: a nitrogen atom with a substituent positioned *Z* experiences more shielding and displays a smaller δ^{15}N value than one with a substituent positioned *E*, while a phosphorus nucleus in a phosphino subtituent positioned *Z* is shielded less and displays a larger δ^{31}P value than one positioned *E*, which is the opposite effect. Based on these considerations, it was concluded that for **1** there probably is a fast *E*,*Z*/*Z*,*E* interconversion, but that the presence of a fraction of *E*,*E* isomer can not be excluded. In the solid state this approach led to the assignment of the *E*,*E* configuration based on the presence of just one singlet in the ^{31}P spectra at a lower shift than in solution.

A number of arguments can be put against these conclusions. One of the reference compounds contained R' = *t*-Bu of which it had been proven that the associated phosphino substituent is virtually permanently fixed in the *E* position, with δ^{31}P 92.4 ppm. For **1** a signal at δ^{31}P 93.2 ppm is found and assigned as an average value of *E* and *Z* even though the difference is very small, at least smaller than the range in which, according to ref. 25, the signal of a phosphorus nucleus positioned *E* should be found (between 82.4 and 92.4 ppm). Furthermore, the authors claimed that only very bulky substituents are capable of forcing systems such as **1** into their *E*,*E* configuration [14], even though the considerably steric manganese complex [Cp(CO)$_2$Mn]R$_2$P–N=S=N–PR$_2$[Mn(CO)$_2$Cp] displays the *Z*,*E* configuration in the solid state [14]. Why **1** should be present in solution at least partially in the *E*,*E* configuration can not be explained by this reasoning.

To assess these trends and their applicability to this kind of configurational assignment, the ^{15}N and ^{31}P chemical shifts were calculated for all conformers and isomers of **3**, and the results are summarized in Table 4. These results indicate that chemical shifts are an unreliable technique to determine the configuration of **1** in solution: for example, the difference in δ^{15}N between gEEg^s and sEEs (both with only S=N bonds in the *E* configuration) is of the same order of magnitude as the difference between the δ^{15}N values of the two nitrogen nuclei in gZEg (with one nitrogen atom in an *E*-S=N bond and one in a *Z*-S=N bond). Although the relation between the configuration of the S=N bond and the relative value of δ^{15}N holds within the same molecule, these values cannot be com-

pared between different conformers, isomers or molecules. The results for the δ^{31}P values are analogous: the value of δ^{31}P of gZZg is *higher* than those of the three most stable *E,E* isomers but *lower* than that of sEEs, whilst the difference in chemical shift between the two phosphorus atoms in the lowest-energy *Z,E* isomer is much larger than any of the differences between the *Z,Z* and *E,E* isomers.

The fact that the dominant configuration in solution of **1** (and **3**) is not *Z,E* but *Z,Z* can be used to fully understand why no indications for the non-equivalence of the two phosphorus atoms, such as splitting or broadening of the signal, could be found down to –100 °C [23], even though these effects *were* observed for the related compound $^{t}Bu_2P–N=S=N–PPh_2$ [24]; indeed, under the assumption that the *Z,E* isomer is energetically favoured, this observation cannot be readily explained. However, using the energies calculated for **3**, an equilibrium composition at –100 °C of 95% gZZg, 3% gZEg^{a}, 1% gZEg^{s} and 1% gZEs is found, giving rise to a single ^{31}P NMR singlet in solution, in agreement with the experimental results; the signals of the other three conformers are very close to or below the detection limit of the technique. The ^{31}P singlet in the solid most likely points to the presence of the (far more energetically favourable) *Z,Z* configuration, which does yield a ^{31}P shift at a lower value than the (average) signal in solution.

3.3. $Me_2P–N=S=N–PMe_2$ (3) and related structures

A comparison of the calculated geometry of the *Z,Z* isomer of **3** with those of previously studied compounds Ph–X–N=S=N–X–Ph [X = S (**2**), Se (**6**)] [10] at the same level of theory is summarized in Table 5. The geometrical parameters and related Hirshfeld bond orders of **3** are generally comparable with those of its –SPh (**2**) and –SePh (**6**) analogues and the bonding in **3** can be described by two localized double S=N bonds and virtually single P–N bonds. The largest differences are found for the P…P distance, which is more than 0.2 Å larger than the S…S and Se…Se distances, and for the PNS angle, which is about 5° larger than the corresponding angles in **2** and **6**. Consequently, whereas the S…S and Se…Se distances are well below the sum of the van der Waals radii [48] (3.60 Å and 3.80 Å, respectively), the P…P distance is above that value (3.60 Å). This suggests that any intramolecular through-space P…P interaction stabilizing the *Z,Z* configuration of **3** is even weaker than those found for Ph–S–N=S=N–S–Ph (**2**) and Ph–Se–N=S=N–Se–Ph (**6**) [10]. This is supported by a topological analysis of the electron density, the results of which, in particular the (3,–1) bond critical points (BCPs) indicating bonding interactions between atoms, have also been collected in Table 5. They show that there is a P…P interaction in the *Z,Z* isomer but that it is extremely weak: the electron density in the BCP is about 26 times lower than the value obtained for the P–N bonds. The corresponding values for Ph–X–N=S=N–X–Ph (X = S, Se) [10] corroborate the conclusions drawn from the geometrical parameters.

3.4. $Me_2P–N=S=N–AsMe_2$ (4)

Replacement of one of the phosphorus atoms in **3** by arsenic lowers the symmetry and increases the number of possible isomers and conformers of **4**, and after optimization of the various possibilities the thirteen structures given in Table 1 remained. From their relative energies it is clear that gZZg remains energetically the most favourable. Six *Z*,*E* and *E*,*Z* isomers lie less than 7 kJ.mol^{-1} higher, while two more, an additional *Z*,*Z* isomer and three *E*,*E* isomers have relative energies of more than 20 kJ.mol^{-1}. Based on these values the equilibrium conformer composition at 293 K for **6** is 50% gZZg, 21% gZEs, 9% gEZg^a, 6% gZEg^a, 5% sEZg, 5% gEZg^s and 4% gZEg^s. It is logical that the contribution of the *Z*,*Z* isomer becomes smaller when more possible *E*,*Z* and *Z*,*E* isomers become available, but the shift in the equilibrium in favour of *E*,*Z* and *Z*,*E* may also be linked to the presence of the heavier arsenic atom. Indeed, while for Ph–S–N=S=N–S–Ph (**2**) the *Z*,*Z* isomer is the main component in solution (about 90%), for its selenium congener Ph–Se–N=S=N–Se–Ph (**6**) this contribution is reduced to less than 50% [10].

The two conformers labelled gEZg^s and gZEg^s are related to the lower-energy structures with the gEZg^a and gZEg^a labels, respectively. Again, the destabilization associated with both groups being located at the same side of the molecule is small: 1.38 kJ.mol^{-1} for gEZg and 1.17 kJ.mol^{-1} for gZEg. Within the set of lowest-energy isomers and conformers of **4** the relative stabilization of gZEs with respect to gZEg, when compared to the situation for **3**, is interesting to note, considering that the relative energy of gZEg changes by less than 0.5 kJ.mol^{-1} between **3** and **4** (Table 1). If the destabilization of the gZEs conformer of **3** is due to the repulsion between the P5 lone pair and the S3–N4 bond, as was mentioned above, then replacement of phosphorus by arsenic and increasing the length of the relevant N–X bond from 1.770 Å in **3** (X = P) to 1.921 Å in **4** (X = As) logically leads to reduced repulsion and increased stabilization. The fifth conformer (sEZg) is associated with the second (gZEs) as the *Z* configuration and *gauche* conformation at phosphorus, and the *E* configuration and *syn* conformation at arsenic in gZEs have been switched in sEZg. The latter is 3.36 kJ.mol^{-1} higher in energy than the former and this destabilization is due to the phosphorus in the "sE" position on the –N=S=N– fragment, which is disfavoured more than when the arsenic atom is in the "Es" position. Likewise, the relative energies of the gEZg^a and gZEg^a conformers indicates that arsenic in the "Eg" position leads to greater destabilization than phosphorus in the "gE" position, but the effect is smaller, as the difference is limited to less than 1 kJ.mol^{-1}. This effect is also expressed in the geometries of the different isomers and conformers presented in Table 6, as the N–As bond lengths show significantly less variation than the N–P distances: going from Eg to Es induces a change of about 0.050 Å in N–P, but only 0.025 Å in N–As. The fact that there is less X–N lone pair repulsion in **4**-gEZa than in **3**-aZEg may also be partly responsible for the relative stabilization of the former compared to the latter.

The geometrical data of the seven lowest-energy isomers and conformers of **4** given in Table 6 can be directly compared to the corresponding parameters of **4** in Table 2. General trends in bond lengths, including shorter *Z*-S=N bonds *vs.* longer *E*-S=N bonds, angles and dihedral angles can be clearly seen. One interesting difference concerns the P…As distance in gZZg of **4** (3.665 Å) which is only just above the sum of the van der Waals radii of phosphorus and arsenic (3.65 Å [49]), but considerably closer to it (the difference is only 0.015 Å) than what was found for the same isomer of **3** (the difference amounts to 0.133 Å), suggesting a stronger interaction in the former. This is corroborated by an analysis of the electron density which produces a value of 0.0074 au at the BCP, which is indeed higher than the value of **3** (0.0058 au, Table 5) and closer to those for Ph–X–N=S=N–X–Ph (X = S, Se) in Table 5. This stronger interaction may again be linked to the presence of the heavier arsenic atom, as the value for Ph–Se–N=S=N–Se–Ph (0.0099 au) is higher than that for Ph–S–N=S=N–S–Ph (0.0078 au).

4. Conclusions

The molecular structures and spectroscopic properties of $^{t}Bu_2P$–N=S=N–$P^{t}Bu_2$ (**1**) and $^{t}Bu_2P$–N=S=N–$As^{t}Bu_2$ (**5**) were investigated using the results of quantum chemical calculations on their dimethyl derivatives **3** and **4** by considering a combination of energetic, structural (geometries and bond orders), electronic (analysis of the electron density) and spectroscopic properties. Me_2P–N=S=N–PMe_2 (**3**) displays a molecular and electronic structure which is similar to those of its chalcogeno derivatives Ph–S–N=S=N–S–Ph (**2**) and Ph–Se–N=S=N–Se–Ph (**6**) in terms of the localization of the double SN bonds and the increased stability of the *Z*,*Z* isomer, but differs from them as the interaction between the peripheral atoms of the XNSNX chain has become weaker for X = P than for X = S,Se. The introduction of the arsenic atom in Me_2P–N=S=N–$AsMe_2$ (**4**) mirrors the changes seen when going from Ph–S–N=S=N–S–Ph (**2**) to Ph–Se–N=S=N–Se–Ph (**6**) as the P…As interaction increases slightly in strength.

5. Acknowledgements

This research was performed within the framework of COST Action CM0802. The authors gratefully acknowledge Prof. Dr. Christian Van Alsenoy for the many helpful discussions and his continued support.

6. References

[1] T. Chivers, *A Guide to Chalcogen-Nitrogen Chemistry*; World Scientific, 2005.

[2] A.J. Banister, I.B. Gorrell, Adv. Mater. 10 (1998) 1415.

[3] M.M. Labes, P. Love, L.F. Nichols, Chem. Rev. 79 (1979) 1.

[4] A.V. Zibarev, A.O. Miller, Yu.V. Gatilov, G.G. Furin, Heteroat. Chem. 1 (1990) 443.
[5] J.M. Rawson, J.J. Longridge, Chem. Soc. Rev. 26 (1997) 53.
[6] A. Modelli, N. Ventura, F. Scagnolari, M. Contento, D. Jones, J. Phys. Chem. A 105 (2001) 219.
[7] R.C. Mawhinney, J.D. Goddard, J. Mol. Struct. (Theochem) 856 (2008) 16.
[8] M. Zahedi, S. Shahbazian, S. Weng Ng, J. Mol. Struct. (Theochem) 629 (2003) 91.
[9] M. Zahedi, S. Shahbazian, S. Weng Ng, J. Mol. Struct. (Theochem) 636 (2003) 229.
[10] K. Tersago, M. Mandado, C. Van Alsenoy, I.Yu. Bagryanskaya, M.K. Kovalev, A.Yu. Makarov, Yu.V. Gatilov, M.M. Shakirov, A.V. Zibarev, F. Blockhuys, Chem. Eur. J. 11 (2005) 4544.
[11] K. Tersago, I.Yu. Bagryanskaya, Yu.V. Gatilov, S.A. Gromilov, A.Yu. Makarov, M. Mandado, C. Van Alsenoy, A.V. Zibarev, F. Blockhuys, Eur. J. Inorg. Chem. (2007) 1958.
[12] A.G. Makarov, I.Yu. Bagryanskaya, Yu.V. Gatilov, N.V. Kuratieva, A.Yu. Makarov, M.M. Shakirov, A.V. Alexeyev, K. Tersago, C. Van Alsenoy, F. Blockhuys, A.V. Zibarev, Eur. J. Inorg. Chem. (2010) 4801.
[13] M. Herberhold, W. Bühlmeyer, A. Gieren, T. Hübner, J. Wu, J. Organomet. Chem. 321 (1987) 51.
[14] M. Herberhold, W. Bühlmeyer, A. Gieren, T. Hübner, J. Organomet. Chem. 321 (1987) 37.
[15] T. Chivers, C. Lensink, J. Richardson, J. Organomet. Chem. 325 (1987) 169.
[16] T. Chivers, C. Lensink, J.F. Richardson, Phosphorus Sulfur Relat. Elem. 30 (1987) 189.
[17] T. Chivers, C. Lensink, J.F. Richardson, Organometallics 5 (1986) 819.
[18] B. Wrackmeyer, E. Kupce, S.M. Frank, S. Gerstmann, M. Herberhold, Phosphorus Sulfur Silicon Relat. Elem. 69 (1992) 179.
[19] M. Herberhold, S.M. Frank, B. Wrackmeyer, B. J. Organomet. Chem. 410 (1991) 159.
[20] W. Ehrenreich, M. Herberhold, G. Herrmann, G. Suess-Fink, A. Gieren, T. Huebner, J. Organomet. Chem. 294 (1985) 183.
[21] A. Gieren, T. Huebner, M. Herberhold, K. Guldner, G. Suess-Fink, Z. Anorg. Allg. Chem. 538 (1986) 21.
[22] M. Herberhold, K. Schamel, Z. Naturforsch. B 43 (1988) 1274.
[23] M. Herberhold, W. Ehrenreich, K. Guldner, Chem. Ber. 117 (1984) 1999.
[24] M. Herberhold, S.M. Frank, B. Wrackmeyer, Z. Naturforsch. B 43 (1988) 985.
[25] B. Wrackmeyer, S. Gerstmann, M. Herberhold, Magn. Res. Chem. 31 (1993) 499.
[26] T. Maaninen, H.M. Tuononen, K. Kosunen, R. Oilunkaniemi, J. Hiitola, R. Laitinen, T. Chivers, Z. Anorg. Allg. Chem. 630 (2004) 1947.
[27] M. Herberhold, W. Ehrenreich, A. Gieren, H. Betz, T. Hübner, Chem. Ber. 118 (1985) 1476.

[28] J. Leitch, S.C. Nyburg, D.A. Armitage, M.J. Clark, J. Cryst. Mol. Struct. 3 (1973) 337.
[29] F.P. Olsen, J.C. Barrick, Inorg. Chem. 12 (1973) 1353.
[30] A. Gieren, H. Betz, T. Huebner, V. Lamm, M. Herberhold, K. Guldner, Z. Anorg. Allg. Chem. 513 (1984) 160.
[31] M.J. Frisch, G.W. Trucks, H.B. Schlegel, G.E. Scuseria, M.A. Robb, J.R. Cheeseman, G. Scalmani, V. Barone, B. Mennucci, G.A. Petersson, H. Nakatsuji, M. Caricato, X. Li, H.P. Hratchian, A.F. Izmaylov, J. Bloino, G. Zheng, J.L. Sonnenberg, M. Hada, M. Ehara, K. Toyota, R. Fukuda, J. Hasegawa, M. Ishida, T. Nakajima, Y. Honda, O. Kitao, H. Nakai, T. Vreven, J.A. Montgomery, Jr., J.E. Peralta, F. Ogliaro, M. Bearpark, J.J. Heyd, E. Brothers, K.N. Kudin, V.N. Staroverov, R. Kobayashi, J. Normand, K. Raghavachari, A. Rendell, J.C. Burant, S.S. Iyengar, J. Tomasi, M. Cossi, N. Rega, J.M. Millam, M. Klene, J.E. Knox, J.B. Cross, V. Bakken, C. Adamo, J. Jaramillo, R. Gomperts, R.E. Stratmann, O. Yazyev, A.J. Austin, R. Cammi, C. Pomelli, J.W. Ochterski, R.L. Martin, K. Morokuma, V.G. Zakrzewski, G.A. Voth, P. Salvador, J.J. Dannenberg, S. Dapprich, A.D. Daniels, Ö. Farkas, J.B. Foresman, J.V. Ortiz, J. Cioslowski, D.J. Fox, Gaussian 09 Revision A.02. Gaussian Inc., Wallingford CT, 2009.
[32] P.J. Stephens, F.J. Devlin, C.F. Chabalowski, M.J. Frisch, J. Phys. Chem. 98 (1994) 11623.
[33] K. Raghavachari, J.S. Binkley, R. Seeger, J.A. Pople, J. Chem. Phys. 72 (1980) 650.
[34] A.D. McLean, G.S. Chandler, J. Chem. Phys. 72 (1980) 5639.
[35] A.J.H. Wachters, J. Chem. Phys. 52 (1970) 1033.
[36] P.J. Hay, J. Chem. Phys. 66 (1977) 4377.
[37] K. Raghavachari, G.W. Trucks, J. Chem. Phys. 91 (1989) 1062.
[38] F.J. London, Phys. Radium 8 (1937) 397.
[39] R. McWeeny, Phys. Rev. 126 (1962) 1028.
[40] R. Ditchfield, Mol. Phys. 27 (1974) 789.
[41] K. Wolinski, J.F. Hinton, P. Pulay, J. Am. Chem. Soc. 112 (1990) 8251.
[42] J.R. Cheeseman, G.W. Trucks, T.A. Keith, M.J. Frisch, J. Chem. Phys. 104 (1996) 5497.
[43] K. Tersago, J. Van Droogenbroeck, C. Van Alsenoy, W.A. Herrebout, B.J. van der Veken, S.M. Aucott, J.D. Woollins, F. Blockhuys, Phys. Chem. Chem. Phys. 6 (2004) 5140.
[44] R.F.W. Bader, *Atoms in Molecules: A quantum theory*; Oxford University Press, 1990.
[45] F. Biegler-König, J. Schönbohm, D. Bayles, J. Comput. Chem. 22 (2001) 545.
[46] F. Biegler-König, J. Schönbohm, J. Comput. Chem. 23 (2002) 1489.
[47] J. Oláh, F. Blockhuys, T. Veszprémi, C. Van Alsenoy, Eur. J. Inorg. Chem. (2006) 69.
[48] A. Bondi, J. Phys. Chem. 68 (1964) 441.

Table 1. Calculated relative energies (ΔE in kJ.mol^{-1}) and symmetries of the nine isomers and conformers of **3** and the thirteen isomers and conformers of **4**; see text for details.

3		**Δ*E***	**4**		**Δ*E***
gZZg	C_2	0.00	gZZg	C_1	0.00
gZEg^a	C_1	4.77	gZEs	C_1	2.16
gZEg^s	C_1	6.42	gEZg^a	C_1	4.21
gZEs	C_1	6.55	gZEg^a	C_1	5.12
aZEg	C_1	30.19	sEZg	C_1	5.52
gEEs	C_1	35.66	gEZg^s	C_1	5.59
gEEg^a	C_2	36.15	gZEg^s	C_1	6.29
gEEg^s	C_s	36.37	gEZa	C_1	22.57
sEEs	C_{2v}	37.47	sEZa	C_s	24.48
			gZZa	C_1	30.03
			gEEs	C_1	31.08
			sEEs	C_s	31.87
			sEEg	C_1	35.77

Table 2. Comparison of the calculated frequencies (in cm^{-1}) of the symmetrical and asymmetrical N=S stretching modes in all conformers and isomers of **3** with the experimental ones (Nujol).

	3	**gZZg**	**gZEg^a**	**gZEg^s**	**gZEs**	**aZEg**	**gEEs**	**gEEg^a**	**gEEg^s**	**sEEs**
ν_{as}	1170	1179	1157	1159	1163	1154	1160	1160	1159	1132
ν_s	1070	1076	1055	1054	1031	1050	1057	1091	1091	1068

Table 3. Selected geometrical parameters of the nine isomers and conformers of **3**; distances in Å and angles in degrees.

	gZZg	**gZEg^a**	**gZEg^s**	**gZEs**	**aZEg**	**gEEs**	**gEEg^a**	**gEEg^s**	**sEEs**
P1–N2	1.734	1.727	1.727	1.728	1.756	1.717	1.716	1.716	1.776
N2=S3	1.552	1.549	1.548	1.542	1.543	1.545	1.552	1.552	1.554
S3=N4	1.552	1.564	1.565	1.572	1.562	1.563	1.552	1.552	1.554
N4–P5	1.734	1.720	1.721	1.770	1.722	1.770	1.716	1.716	1.776
P...P	3.733	4.985	4.986	5.064	5.220	5.753	5.833	5.823	5.669
P1–N2–S3	134.2	128.5	129.0	129.3	135.4	129.2	128.7	128.7	116.6
N2–S3–N4	124.2	114.8	115.0	114.4	117.6	110.4	110.5	110.5	110.2
S3–N4–P5	134.2	128.8	128.4	116.9	128.5	115.7	128.7	128.7	116.6
P1–N2–S3–N4	5.7	-11.6	-11.4	10.6	-0.5	171.5	-167.1	-171.4	180.0
N2–S3–N4–P5	5.7	-171.2	172.3	-179.7	171.4	179.2	-167.1	171.4	180.0

Table 4. Calculated ^{31}P and ^{15}N NMR chemical shifts (in ppm relative to H_3PO_4 and CH_3NO_2, respectively) of all conformers and isomers of **3**. For comparison, the experimental values of **1** are included (measured at room temperature in CD_2Cl_2 and C_6D_6, respectively [24,25]).

	1	**gZZg**	**gZEg^a**	**gZEg^s**	**gZEs**	**aZEg**	**gEEs**	**gEEg^a**	**gEEg^s**	**sEEs**
P1	93.2	49.0	64.7	63.6	66.4	52.5	47.3	47.0	47.2	54.1
P5	93.2	49.0	49.8	49.9	45.1	50.6	48.6	47.0	47.2	54.1
N2	-58.1	-24.1	-51.2	-53.4	-35.3	-65.9	24.3	11.3	6.2	70.6
N4	-58.1	-24.1	14.2	13.1	52.1	52.1	53.9	11.3	6.2	70.6

Table 5. Selected calculated (B3LYP/6-311+G*) geometrical parameters of the lowest-energy isomers of three R–N=S=N–R; bond lengths in Å, angles in degrees. Hirshfeld bond orders (BO) are given for the bonded distances; values of the electron density ρ(*r*) (in a.u.) are given for the relevant BCPs.

	–PMe$_2$ (3)			**–SPh (2)**			**–SePh (6)**		
		BO	ρ(*r*)		**BO**	ρ(*r*)		**BO**	ρ(*r*)
X1–N2	1.734	1.20	0.1505	1.688	1.25	0.2012	1.851	1.03	0.1508
N2–S3	1.552	2.02	0.2537	1.571	1.81	0.2445	1.566	1.85	0.2483
X...X	3.733		0.0058	3.471		0.0078	3.523		0.0099
X1–N2–S3	134.2			129.3			128.5		
N2–S3–N4	124.2			124.7			125.7		
X1–N2–S3–N4	5.7			-3.3			-3.6		

Table 6. Selected geometrical parameters of the seven lowest-energy isomers and conformers of **4**; distances in Å and angles in degrees.

	gZZg	**gZEs**	**gEZg^{a}**	**gZEg^{a}**	**sEZg**	**gEZg^{s}**	**gZEg^{s}**
P1–N2	1.739	1.729	1.722	1.728	1.770	1.724	1.729
N2=S3	1.553	1.545	1.563	1.549	1.570	1.563	1.548
S3=N4	1.549	1.568	1.546	1.562	1.539	1.545	1.562
N4–As5	1.900	1.921	1.898	1.895	1.902	1.899	1.895
P...As	3.665	5.223	4.975	5.188	5.061	4.974	5.176
P1–N2–S3	132.8	129.0	129.1	128.6	117.3	128.5	128.7
N2–S3–N4	124.9	114.9	115.4	115.1	115.0	115.6	115.2
S3–N4–As5	131.1	115.8	124.3	123.0	124.8	124.6	123.0
P1–N2–S3–N4	-6.3	10.6	172.5	10.8	179.1	-171.3	-11.5
N2–S3–N4–As5	-3.0	-179.7	9.0	173.3	-8.3	9.1	173.5

Figure 1. The four possible configurations of asymmetrically substituted sulfur diimides.

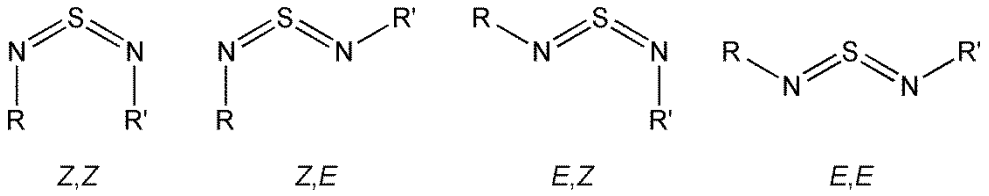

Z,Z *Z,E* *E,Z* *E,E*

Figure 2. Numbering of the atoms and structural formulas of the compounds under investigation.

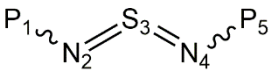

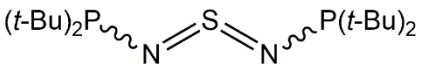

1

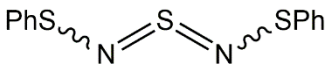

2

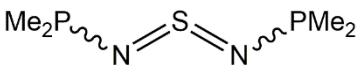

3

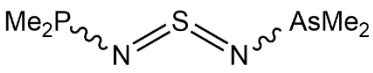

4

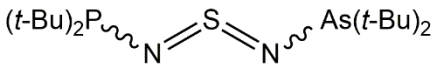

5

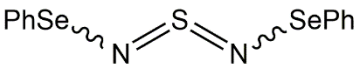

6

Figure 3. Diagrams representing the structures of (a) the gEZg^a and (b) the gEZg^s conformers of **4**; see text for details.

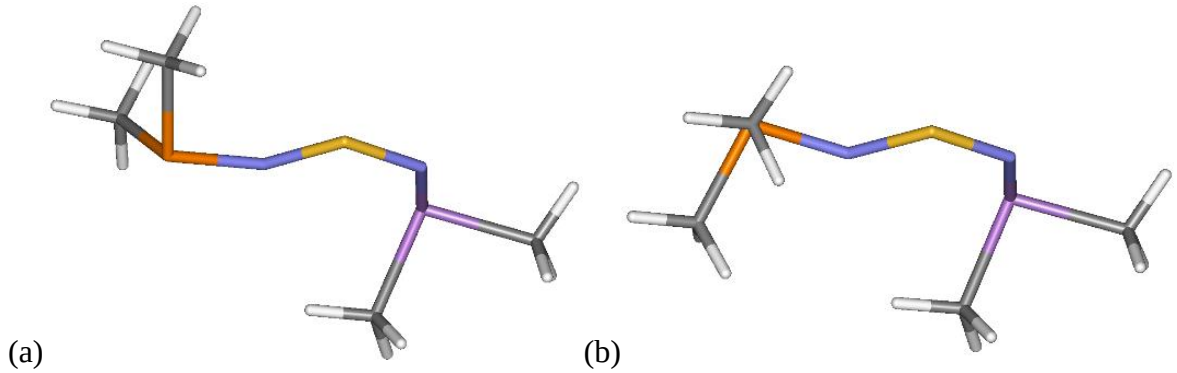

(a) (b)

Figure 4. Diagrams representing the structures of four of the lowest-energy isomers and conformers of **3**: (a) gZZg, (b) gZEg^a, (c) gZEs, and (d) aZEg. The lone pairs on the heteroatoms are represented by the pink spheres (see text for details).